wjpmr, 2019, 5(2), 237-249

SJIF Impact Factor: 4.639

WORLD JOURNAL OF PHARMACEUTICAL AND MEDICAL RESEARCH

www.wjpmr.com

Research Article

ISSN 2455-3301

WJPMR

FUNCTIONAL CONNECTIVITY BETWEEN THE MIDBRAIN AND CORTEX DURING CONSCIOUSNESS RECOVERY AFTER GENERAL ANESTHESIA

Lyubov B. Oknina*[1], Anna O. Kantserova[1,2], Eugeny L. Masherov[3], Vitaly V. Podlepich[3], Oleg S. Zaitsev[3] and David I. Pitskhelauri[3]

[1]Institute of Higher Nervous Activity and Neurophysiology of RAS, Moscow, Russia.
[2]Lomonosov Moscow State University, Moscow, Russia.
[3]N.N. Burdenko National Medical Research Center of Neurosurgery, Moscow, Russia.

***Corresponding Author: Lyubov B. Oknina**

Institute of Higher Nervous Activity and Neurophysiology of RAS, Moscow, Russia.

Article Received on 20/12/2018 **Article Revised on 10/01/2019** **Article Accepted on 31/01/2019**

ABSTRACT

The study aimed to calculate functional connectivity between the cortex and midbrain area (periaqueductal grey, PAG). For this, in 5 patients at the final stage of surgery after removal of the pineal region tumor, the external ventricular drainage with recording devices located at the tip was inserted into the aqueduct. Thus, by draining the cerebrospinal fluid from the ventricular system for therapeutic purposes we could register the local potentials of the periaqueductal region during anesthetic sleep, waking from it and wakefulness. ERPs were recorded simultaneously from deep electrodes located close to intact PAG area and scalp electrodes using auditory two-tone oddball paradigm. The selection of peaks was made in N100, N200 and P300 time windows. Functional connectivity was calculated in time windows including 65 ms before and after peak latency on deep electrode and used in the Granger causality test (value of model order n=10). The peaks recorded on deep electrodes were considered under the same names (N100, N200 and P300) for convenience of description and comparison with those recorded on scalp sites. In clear consciousness ERP was clearly detected on scalp electrodes, as well as peaks on deep electrodes. The changes of direction of functional connectivity were detected during consciousness recovery: the direct connectivity from the frontal area to brainstem was revealed in post-anesthesia disorders of consciousness and obnubilation with the connectivity value greater in post-anesthesia disorders of consciousness, and the direct connectivity from the brainstem to left cortex area was detected in clear consciousness.

KEYWORDS: Functional connectivity, deep electrodes, Granger causality, ERP, consciousness recovery, PAG.

INTRODUCTION

It is beyond argument that the consciousness is a product of the brain with a key role of the cortex (Boly et al. 2017), nevertheless, there is no consensus on the question what type of functional connectivity and between what neurons cohorts provides consciousness and cognition (Hess and Brugger 1943, Adams 1979, Carrive et al. 1989, Beck et al. 2017). Revealing mechanisms of the cortex-subcortex interaction and the role of deep brain structures in consciousness is a field of interest for many studies. There has been a lot of evidence of the role of the brainstem structures in maintaining consciousness since the research of Jasper (1969) and Penfield (1975), using craniotomy and manipulating with patients in consciousness during the operation postulated, that integrative functions are forming not in the cortex but in the rostral area of the brain and about a probable key role of the centrencephalic system in consciousness.

The point of view that the brainstem is crucial to the consciousness was developed by Merker (2006). He supposed that a basic level of consciousness is possible to observe in children with anencephaly.

The role of midbrain-cortex functional interaction in consciosness and cognition has been controversial in the last several years (Philippini et al. 2012). The role of midbrain and, in particular, the periaqueductal gray (PAG) has been ascribed a vast array of functions related to survival and the selection of adaptive behavioral responses (Bandler and Keay 1996, Brandao et al. 1999, Linnman et al. 2012), particularly in the context of maternal care (Lonstein and Stern 1997, Sukikara et al. 2006, Parsons CE et al. 2013.).

Deep located brain areas, including PAG, are “hidden” from direct access of brain activity, therefore, there is no rigorous evidence that the mesencephalon is involved in cognitive activity. The studies, devoted to local field potentials (LFP) recorded from the midbrain, concern

patients with chronic pain syndrome and implanted stimulating electrodes (Nashold et al. 1969, Taira et al. 1987, Parsons et al. 2013). The study of electrophysiological brain oscillations has opened a new window towards the understanding of neural functions. LFPs represent the aggregate activity of small populations of neurons represented by their extracellular potentials. These signals are well suited for use in closed-loop neurophysiology because they are robust, easy to record, and clinically useful. But the previously technically difficult operation of electrode implantation is currently successfully competed with the motor cortex stimulation and implantation of a morphine pump and, therefore, the implantation of deep electrodes in PAG is done very rarely, so the chances to research activity of PAG in human decrease.

The studies reflecting the involvement of PAG in the nociceptive system revealed that this brain area contained a large number of opiate receptors and is connected with the sympathetic nervous system. This structure participates in the forming of pain perception and emotional coloring of nociception and at the same time it is not isolated from other structures, but included in the reciprocal connectivity with the thalamus, motor cortex and spinal cord (Linnman et al. 2012). PAG is involved in forming defense reactions, anxiety, fear and panic that could be connected with serotoninergic neurons located in the raphe nuclei and the ventrolateral part of PAG, and they inhibit the dorsal part of PAG on which the response depends. During the forming of these emotions PAG has connectivity with the cingulate gyrus and hippocampus (Vianna 2001). Moreover, different areas of PAG contribute differently to fear (Vianna 2001, Farook et al. 2004; Parsons 2013). The increasing of PAG activity in human was reported in response to aversive compared to neutral sounds (Zald and Pardo 2002) and voiced compared to unvoiced speech (Schulz et al. 2005). The activity in PAG was also suggested to underlie the pleasurable 'chill' experienced when listening to music (Blood and Zatorre 2001). Thus, the activation of PAG was detected in response to different outside and inside signals and, supposedly, could be activated in consciosness.

Neuronal networks in the human brain are remarkable systems capable of generating complicated patterns of brain functions, such as awareness, attention, memory and self-recognition, and modulating behavior due to the combination of an enormous computational capacity, provided by a huge number of neurons and brain connectivity (Hagmann et al. 2007, Sherwood et al. 2008). To understand the mechanisms behind brain functions and to reveal functional connectivity between neuronal groups involved in brain functions, a detailed study of individual neural cells and small neuronal groups is clearly insufficient (Laughlin and Sejnowski 2003, Koch and Laurent 1999**).** Moreover, a baseline cognitive functional activity, such as awareness, needs to be considered (Boly et al. 2017, Wollstadt et al. 2016).

The network architecture of awareness and some cognitive activity of the entire human brain could be represented by graphs of connectivity between the brainstem and cortex. The most common methods of statistical estimation of relationships, such as correlation or coherence analysis, information-theoretical assessment and others, are symmetric with respect to permutation of their arguments, and the direction of connection cannot be estimated. In some cases, we can distinguish between cause and effect using meaningful considerations, but in others, such as the problem of estimating the interaction of brain structures, that kind of additional information is not available, and there is a need for methods able to distinguish cause from effect. One of those methods is causality measure proposed by the concept of Granger causality developed about fifty years ago and applied to the field of ecomometrics to study the relationships between economic indices. Granger causality allows investigation of direct functional connectivity or statistical dependence among multiple signals (Wiener 1956, Granger 1969).

His basic idea, going back to the works of David Hume, is that the cause precedes its effect and influences the result. Therefore, the evaluation procedure is to construct two models for considered variables; the first model includes only the previous values of simulated variables, while the second, in addition to values of simulated variables, includes the previous values of possible variables considered as the cause. If the second model is more accurate than the first, we can say that the second value is the cause for the first. However, in the case of swapping those variables and conducting a similar procedure, the first may be the cause for the second. When it is impossible to talk about the unidirectional causal relationship, it is either the feedback loop or the presence of a third variable causally related to the first two. Distinguishing between these situations is possible if the third value is both observable and in accordance with the measure of Granger causality. Otherwise, it is only possible to ascertain mutual influence of variables differentiating the presence of the feedback loop or the common cause for the two processes.

The idea of the method allows using different models of the studied processes but due to the difficulty of estimating those models practical implementation is based on the linear autoregression model:

$$y_t = a_0 + a_1 y_{t-1} + a_2 y_{t-2} + \cdots + a_m y_{t-m} + \text{error}_t,$$

For the first variable and

$$y_t = a_0 + a_1 y_{t-1} + a_2 y_{t-2} + \cdots + a_m y_{t-m} + b_p x_{t-p} + \cdots + b_q x_{t-q} + \text{error}_t$$

For the joint effect of the first and second variables. A criterion of causal influence of the second variable on the first is the ratio of the variances of errors in the second and in first models. When previous values of second variable are included in the model the decrease of

variance is considered to be confirmation of the causal influence of the second variable on the first. This procedure is usually carried out with variables being interchanged, allowing the interaction of variables with unidirectional causality and variables without causes and consequences being clearly discriminated to be distinguished. The Fourier transform may be used to compute causality in frequency domain.

The use of Granger causality assumes a priori orders for both models. In terms of simulated spectrum, the number of peaks in a frequency spectrum is limited by half of the order of the model.

In an auxiliary n^{th} degree polynomial equation, each pair of complex roots corresponds to an exponentially decaying sinusoid. Although, an exponentially growing sinusoid or a constant are mathematically possible, the unlimited growth cannot occur in real biological objects. Those components are either absent or manifested only within short periods. The real roots of the auxiliary equations correspond to aperiodic exponential decay.

We wonder whether the midbrain-cortex interaction has a specific role in consciousness and cognition. To test this, we carried out simultaneous recording of brain activity from scalp and deep electrodes, located close to PAG. As a measure of cognitive activity we used event-related potentials (ERP) for simple tones measured in the context of oddball paradigm (Beck et al. 2017). According to the vast number of publications, event-related potentials (ERPs) could be considered as a measure of cognitive functions. P300 is an important event-related potential (ERP) component elicited by infrequent and task-relevant stimuli, and it reflects the processes of attention, stimulus classification, and memory updating. The N100 of ERP reflects perceptual processing stage around 100 ms after stimulus onset determined by physical stimulus properties and, somewhat, is influenced by attention and orienting processes and, supposedly, reflects neural activity in the supratemporal plane, at and around the primary auditory cortex (Naatanen and Picton 1987). By contrast, the P300 reflects higher-level processing stages that are required to evaluate task-relevant events (Verleger 1997, Donchin and Coles 1988, Polich 2007) and reflect activity of sources located over the (dorsolateral) prefrontal cortex and in the parietal lobe, including the superior parietal lobule, the temporoparietal junction and the posterior part of the cingulate gyrus (Knight et al. 1989, Polich 2007, Wronka et al. 2012).

Using dipole source analysis of ERP in patients with brain trauma and consciousness disorders, the role of the brainstem, together with activity of cortex regions was determined (Sharova et al. 1998, Oknina et al. 2011). Intracranial recordings of ERP in humans allowed revealing subcortical structures involved in ERP components generation: the thalamus and basal ganglia, the midbrain reticular formation (Naatanen and Picton 1987, Kropotov and Ponomarev 1991, Rektor et al. 2004, Durschmid et al. 2015).

The present study aimed to calculate functional connectivity between the cortex and brainstem and to explore the involvement of the midbrain (PAG) in consciousness recovery and cognitive activity. The novelty of the study is in simultaneous recording of ERP from deep electrodes located close to the PAG area and scalp electrodes as well as the calculation of Granger causality between the cortex and midbrain during post-anesthesia disorders of consciousness, obnubilation and clear consciousness.

MATERIALS AND METHODS

Participants

Ethical approval of the research methods was obtained from Burdenko Neurosurgery Institute Research Ethics Committee. Participation of patients in study was voluntary and the patients gave written informed consent to take part in the study. The study included 5 patients with tumors of the pineal region who underwent tumor removal by anterior interhemispheric approach. After removal of the tumor at the final stage of the operation a specially developed external ventricular drainage was installed for 24 hours for the purpose of draining cerebrospinal fluid (CSF) and preventing possible CSF circulation disorders. The multi-perforated distal end of the drainage was inserted into the lumen of the aqueduct to the upper sections of the fourth ventricle. The electrodes were mounted at this end of the drainage which were wired inside the drainage tube and connected to the recording device. The diameter of the drainage (2.5 mm) in the aqueduct ensured close contact of the electrodes with the internal surface of the aqueduct in close proximity to PAG. More information about the operation technique is available in the study (Konovalov and Pitskhelauri 2003, Pitskhelauri 2009, 2012). The electrode placement was determined on the basis of computer tomography (CT) imaging.

Brain activity recording started in the intensive care department and lasted for 24 hours after operation. ERPs were recorded in anesthesia disorders of consciousness approximately 5 minutes before awaking (in one patient), immediately after awaking in obnubilation (in one patient), 24 hours later in clear consciousness (in 4 patients) and in obnubilation (in one patient). Consciousness recovery in patients was evaluated by a neuropsychiatrist before, during and after ERP recording.

The characteristics of patients, electrode sites, timing of study and middle latency of intervals to Granger causality calculation (peak latency of N100, N200 and P300) are presented in Table 1.

Table 1: Characteristics of patients, timing of study, and middle latency of intervals to Granger causality calculation of ERP components.

	Gender	Age	Scalp electrodes		Post-anesth. dis. of cons.	1 hour obn./ passive	1 hour obn./ count	12 hours obn./ passive	12 hours obn./ count	24 hours/ clear cons./ passive	24 hours/ clear cons./count
1	M	31	F4, Fz, Cz, P3, P4, Pz,T5, T6, O1, O2	N100 N200 P300		114 ms 204 ms 298 ms	110 ms 212 ms 312 ms			84 ms 200 ms 310 ms	106 ms 206 ms 310 ms
2	F	25	Fp1, Fp2, C3, C4, P3, P4, O1, O2, T5, T6	N100 N200 P300	106 ms 236 ms 306 ms						88 ms 150 ms 310 ms
3	M	21	F3, F4, Cz, P3, P4, T6, O1	N100 N200 P300						65 ms 204 ms 295 ms	88 ms 198 ms 294 ms
4	F	27	Fp1, Fp2, F3, F4, F7, F8, Fz, C3, C4, Cz, T5, T6, P3, P4, Pz,T5, T6, O1, O2	N100 N200 P300				114 ms 216 ms 304 ms	110 ms 210 ms 334 ms		
5	M	24	Fp1, Fp2, C3, C4, P3, P4, T5, T6	N100 N200 P300							110 ms 176 ms 310 ms

Control group. As a brain signal from the deep electrode was impossible to record in healthy subjects, we were to focus on individual changed of ERPs recorded on deep electrodes during consciousness recovery. ERPs from scalp electrodes were recorded in 24 healthy subjects aged 18-59.

Stimulus presentation: The participants performed an auditory two-tone oddball paradigm (Polich 2007). A total of 100 stimuli were presented in one experimental block, including frequent standard stimuli (probability of occurrence 80%, 800 Hz, 80 ms) and infrequent deviant stimuli (probability of occurrence 20%, 600 Hz, 80 ms). Tones were presented binaurally through earphones.

ERPs under anesthesia were recorded in passive conditions, e.g. without any instruction. For patients in obnubilation and in clear consciousness, ERPs were recorded in two blocks. The first block included ERP-recording without any instruction (passive block). In the second block the patients were given an instruction to count rare (deviant) tones.

Electrophysiological recording

All the recordings were conducted using Neurobotics system, Russia. Simultaneous recording were obtained from the scalp surface and deep brain PAG region. Scalp brain potentials were recorded from electrodes located by the 10-20% system. The number of electrodes varied from 8 to 19 and depended on a possibility to site electrodes in the intensive care department.

Local potentials were recorded from two electrodes located in the cerebral aqueduct close to PAG. The scheme of notch drainage-electrode is presented in Figure 1. The length of deep electrodes was 10 mm. The distance between two electrodes was 2,5 mm.

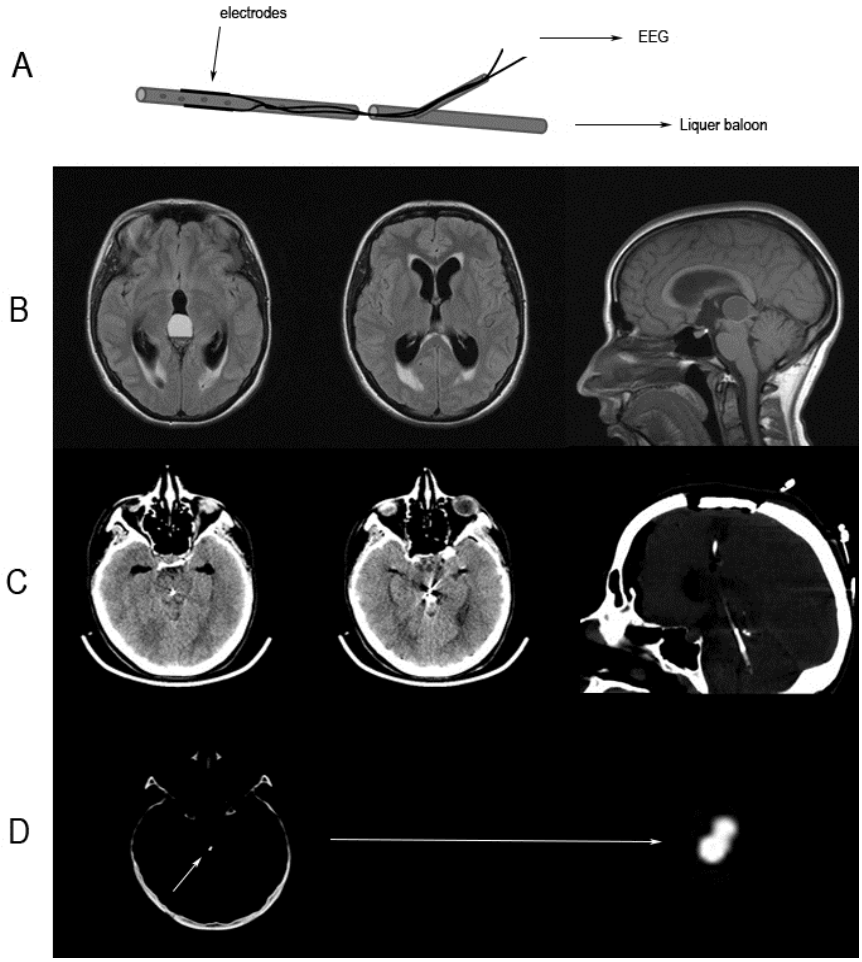

Figure 1: A - scheme of notch drainage-electrode. Drainage-electrode uses two independent functions: treatment – remove spinal fluid out of ventricular system of brain, control of homeostasis in a bed of removed tumor, diagnostics – record brain activity from deep brain area; B – cist of pineal area located in posterior part of third ventricle of brain and leading to occlusion hydrocephaly. The transcallosal subchotoidal approach for resection of tumor was used and drainage-electrode set; C - CT-control after operation with location of electrodes in aqueductus cerebry and forth ventricle of brain; D – on increased part of CT the orientation of electrodes to colliculus and mesencephalic tegmentum.

Both signals were recorded using an online analog notch filter; a high-pass filter was 0,5 Hz and a low-pass filter, with a cutoff frequency 70 Hz. Real time filters were applied to get immediate feedback of data quality.

Data analysis

Brain signals were analyzed with MATLAB (R2015b, Math Works, USA) Brainstorm toolbox (Tadel et al. 2011) and Neurobotics (Russia).

Artifact correction. Initially, band-pass filters (0,5-70 Hz) and frequency filters were used to run the 50 Hz notch. Additionally, the manual rejection of artifacts, such as movement or skin-reaction, was done.

The time domain of responses for each type of stimuli was averaged separately. The averaged response included 100 ms pre-stimulus of a baseline signal and 800 ms of a post-stimulus signal.

The selection of peaks of the averaged response was made in areas of interest including the N100 (55 to 120 ms), N200 (150 to 300 ms) and P300 (200 to 400 ms) time windows. Taking into account changes of consciousness in patients, the time windows were wider than conventional ones. The time values of signals from all the sites for every patient in each state of consciousness were put on the chart in order to identify the peaks. The mean value of peak latency from stem electrodes for each peak was found. The time windows including 65 ms before and after peak latency on deep electrode were calculated and used in the Granger causality test to explore causal interactions (effective connectivity) between the brainstem and different areas of the cerebral cortex. The middle latency of Granger causality intervals for peaks N100, N200 and P300 are presented in Table 1. If peaks were not detected we used time windows with a center on 110 ms, 200 ms and 300 ms as a more typical peak latency for these components.

To estimate connectivity between brain areas Granger causality was used. The value of model order n=10, which implies not greater than five frequency peaks in the spectrum, is widely excepted and used in the BrainStorm software. Bivariate Granger causality was used to calculate connectivity between all possible pairs of sites. The intensity threshes and Distance Filtering parameters we altered to obtain the greatest number of links with an easy to view density. To assess the obtained cortical-brainstem interaction, the bivariate Granger causality graphs were analyzed.

Then we analyzed connectivity between deep and cortex electrodes by calculating the ratio C/A, where C - number of connections with dominant cortical effects and A - total number of directed links): (C/A)*100%. We supposed that if C/A > 50%, the dominant influence of the cortex is revealed; if C/A < 50%, the dominant influence of the brainstem is revealed. Then these ratios were analyzed and compared in every patient for each state of consciousness. Finally, we carried out the comparison of the cortex-cortex links by creating matrices of weight ratios, calculating following factors based on these matrices and comparing them between each other. We calculated

- Sum of weight ratios reflects the influence of the cortex of right hemisphere on the cortex of left hemisphere minus sum of weight ratios reflects the influence of the cortex of left hemisphere on the cortex of right hemisphere (CR->CL);
- Sum of weight ratios reflects the influence of the frontal cortex on the parietal cortex minus the sum of weight ratios reflects the influence of the parietal cortex on the frontal cortex (Fr->P);
- Sum of weight ratios reflects the influence of the frontal cortex on the temporal cortex minus sum of weight ratios reflects the influence of the temporal cortex on the frontal cortex (F->T);
- Sum of weight ratios reflects the influence of the temporal cortex on the parietal cortex minus sum of weight ratios reflects the influence of the parietal cortex on the temporal cortex (T->P).

In matrices, frequencies of occurrence of links were determined as weight ratios. The factors (CR->CL, F->P, F->T, T->P) were averaged by peaks and by patients and then compared between each other by states of consciousness. Also, we introduced directed graphs in order to identify the most influential and dependent sensors in each state of consciousness. Furthermore, we used directed volumetric graphs in the model a head to assess the distribution of links and direction of causality.

RESULTS

Behavior task

In clear consciousness all the subjects performed the task according to the instructions. They responded with high accuracy to the target stimulus. In obnubilation one patient performed the task, whereas another patient counted frequent tones instead of rare ones.

Electrophysiological data

The N100, N200 and P300 peaks were clearly detected on scalp sites. On deep electrodes the peaks with latency around considered time intervals were also revealed. These deep peaks went under the same names (N100, N200 and P300) for convenience of description and comparison with those recorded on scalp sites. The responses recorded on deep electrode and parietal scalp electrodes in post-anesthesia disorders of consciousness, obnubilation and clear consciousness are presented in figure 2.

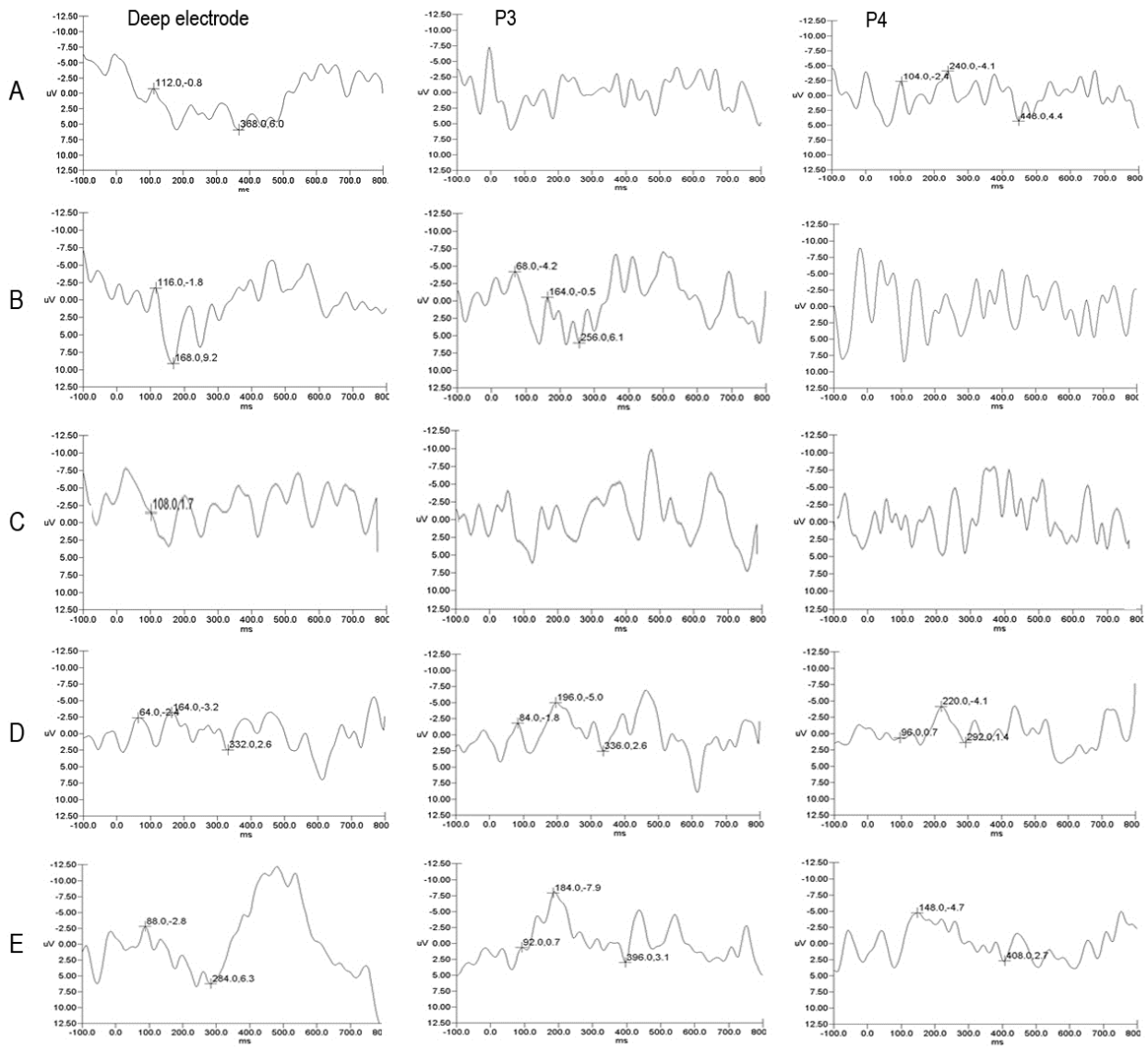

Figure 2: ERPs recorded on deep electrode, P3 and P4 sites (the sites were selected so these electrodes were in all patients). Amplitude and latency is presented only for peaks which were considered as elicited. A – in patient 2 in post-anesthesia consciousness disorders; B – in patient 4 in abnubilation, 12 hours after operation, during listening to tones; C – in patient 4 in abnubilation, 12 hours after operation, with instruction to count target tones; D - in patient 3, in clear consciousness, 12 hours after operation, during listening to tones; E - in patient 3, in clear consciousness, 12 hours after operation, with instruction to count target tones.

In post-anesthesia disorders of consciousness, just before awareness, the elicitation of peaks was better in deep electrodes and the waveform differed from those on scalp. The N100 latency on deep electrodes was longer than on scalp electrodes: 112 ms vs. 104 ms; P300, shorter: 368 ms vs.440 ms. On scalp electrodes, ERP was clearly detected on the right-side sites.

In obnubilation the detection of peaks was complicated. The response was noised by frequent oscillations and disorganized. Only N100 was clearly detected on deep and left-side scalp electrodes during the listening to tones. The latency of N100 was longer on deep electrodes: 116 ms vs. 68 ms. On left-side scalp electrodes, the N200 peaks with latency 164 ms and, supposedly, P300 with latency 256 ms were detected. None of those was revealed on deep electrodes.

The instruction to count target tones leads to disorganization of response. There was no ERP detected.

In clear consciousness ERP was clearly detected on scalp electrodes during the listening to tones. On deep electrodes peaks were also revealed with the same latency as on scalp sites, but they had lower amplitude. ERP recorded in the task of counting tones on scalp electrodes had greater amplitude of N200 and P300 than during the listening to tones. On deep electrodes the changes of waveform were detected. Only two peaks,

supposedly N100 and P300, were detected. Moreover, a negative wave with latency about 500 ms was detected.

Granger causality

We calculated Granger causality between all pairs of sites. But the main attention was paid to links between the brainstem and cortex.

In post-anesthesia disorders of consciousness, the directed links from the frontal area to other cortex regions - in the N100 time range from left temporal sites, in the N200 time range from the right frontal site and in the P300 time range from the left frontal area - were detected.

In obnubilation, the directed links from the left cortex area to brainstem and from the brainstem to left cortex area were revealed.

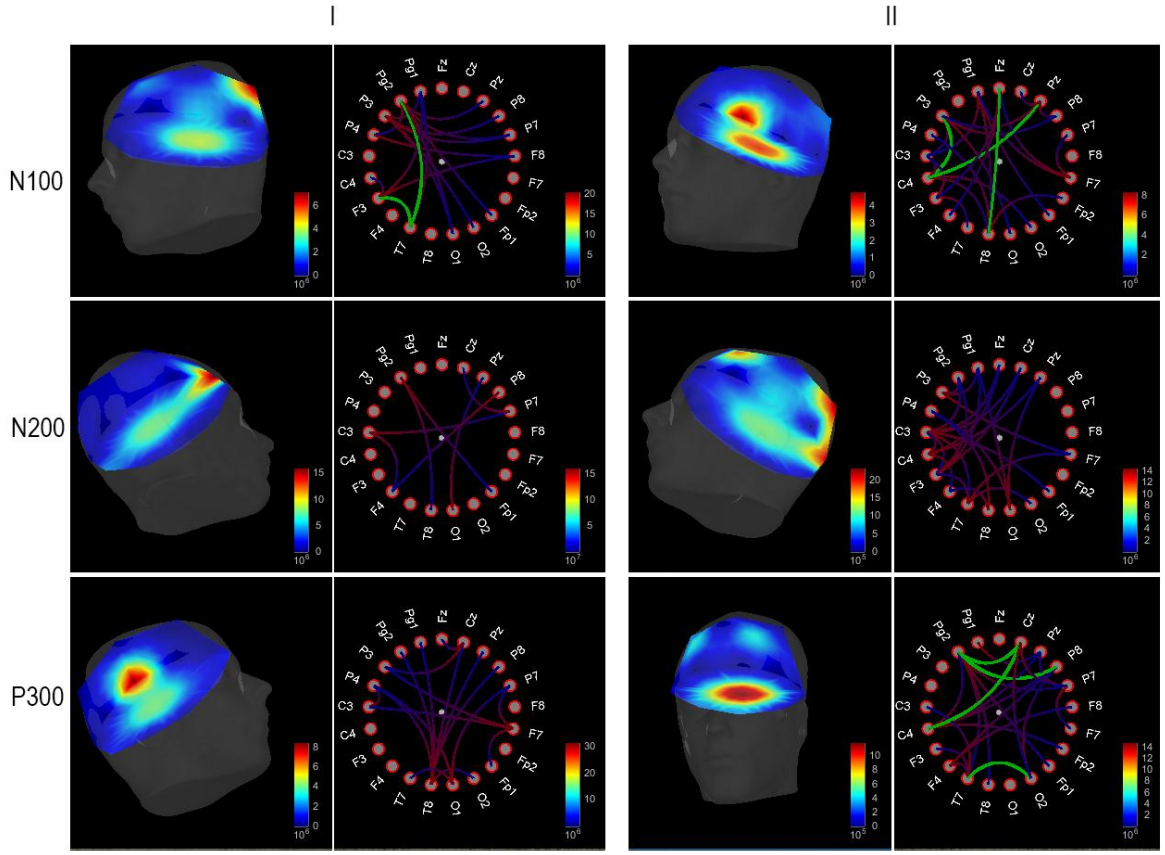

Figure 3: Functional Granger causality in patient 4 in obnubilation, 12 hours after operation, in intervals of 114 ± 65 ms (N100), 216 ± 65 ms (N200) and 304 ± 65 ms (P300) I - during listening to tones, II - with instruction to count target tones. 3-D sensor diagrams show the connectivity between deep electrode and scalp electrodes. The color scale is proportional to effect. In diagrams the connectivity between all possible pairs are present. Green lines show bi-directional links, blue-red lines - directed links. The direction of causality is from red to blue.

The visualization of Granger causality for the patient in obnubilation 12 hours after operation during the listening to tones and counting target tones is presented in Figure 3. The diagrams show the direction and power of causal-consequence interaction between signals recorded on different sites in the N100, N200 and P300 intervals. Green links show bipolar connectivity and red-blue links show directional connectivity with dominant influence from red to blue. The ratio of connectivity with the direction of influence from the cortex to all the connectivity has specificity depending on a patient's functional state.

The number of connectivity was larger in the task of counting and the strength of links was lower on the intervals of N100 and P300.

In clear consciousness, during the listening to sounds, the directed links from frontal to deep electrodes were detected. During the count of target tones the directed and bi-polar links were revealed between the deep and left frontal sites. The value of deep effect was greater, especially for the N200 interval (Figure 4).

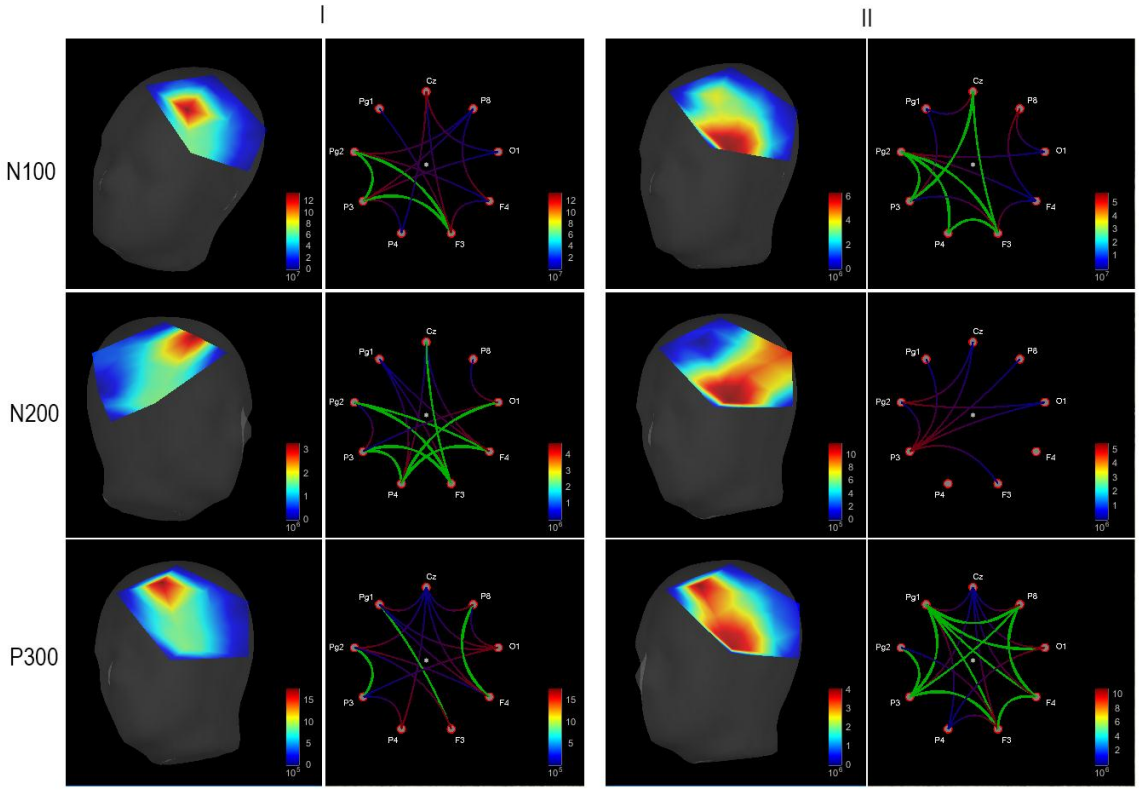

Figure 4: Functional Granger causality in patient 3 in clear consciousness, 24 hours after operation, in intervals of 65 ± 65 ms (N100), 204 ± 65 ms (N200) and 295 ± 65 ms (P300) I - during listening to tones, II - with instruction to count target tones. 3-D sensor diagrams show the connectivity between deep electrode and scalp electrodes. The color scale is as indicated in figure 3.

The analysis of the total effect of all pairs of connectivity revealed that in anesthesia the directed connectivity from right-side scalp electrodes to deep electrode dominated (C/A > 50%). The decrease of C/A ratio was detected as consciousness was being recovered. In obnubilation C/A varied around 50% and in clear consciousness C/A < 50%. It should be noted that in clear consciousness C/A was less during the listening to tones in comparison to counting tones.

Table 2: The value of C/A ratio in different states.

	D->LC	D->RC	D->Fr	D->P	D->T	CR->CL	Fr->P	Fr->T	T->P
anesthesia	-1.140	-0.327	-0.327	-0.217	-0.490	1.399	0.000	-0.300	0.133
obnubilation	-0.137	0.129	-0.015	0.096	0.149	-0.036	0.086	0.028	0.073
consiousness	-0.188	0.035	-0.158	0.102	-0.192	-0.110	0.130	0.008	0.151

D- deep electrodes, LC – left scalp sites, RC – right scalp sites, Fr – scalp frontal sites, P – scalp parietal sites, T – scalp temporal sites. Dominant direct effect has positive value. Inverse dominant value has negative value.

We summarized directed influence between the deep-cortex and cortex-cortex areas in different states of consciousness in Table 2.

DISCUSSION

Limitation of the study

In the study the activity of deep intact brain structures is contrasted to the majority of research using a recording deep electrode combined with a deep stimulating electrode. As the number of patients was not sufficient to rigorous statistical analysis, the focus was made on the analysis of individual data.

We recorded brain activity simultaneously from the scalp and deep located brain structures, supposedly from PAG. PAG is not a part of a simple reflex arc but is a primary center reacting to stress, anxiety, life threat and, according to indirect evidence contributes to cognitive activity (Jasper 1969, Penfield 1975, Strehler 1991, Parvazi and Damasio 2001, Merker 2007).

Oscillations recorded from deep electrodes have similar nature as those recorded in the LFP (local field potentials) paradigm. They, as well as LFP, reflect oscillations and action potentials of neurons located close to electrode. There are some specifications used in acquisition of signals that influence the area from which

a local signal is recorded. This forces us to reject the definition 'local' and use only 'field potentials' (Herreras 2016). LFP is generally recorded using bipolar montage with distance between electrodes up to 5 mm that allows determining a signal as 'local', although the problem of contribution activity of the more remote structures is discussed (Kajikawa and Schroeder 2011, Whitmore and Lin 2016). In our study this problem is principal because the recording of brain signals was done using ear indifferent electrodes, which is more typical for clinical study.

The calculation of influence of brain structures activity depending on distance to recorded signal requires information about the electrical properties of brain tissues, first of all, conductivity. The rough estimation could be obtained if sources of activity are considered as dipoles evenly distributed in the brain with occasional orientation according to the Bienaymé formula for variance of the sum of uncorrelated variables (Loeve 1977). The potential created in the point by dipole is inversely proportional distance r from dipole to point squared. The square of a spherical layer of known thickness with radius r and center in the point and, consequently, the number of dipole sources in the layer are proportional to r squared. The summarized potential, due to the hypothesis of independence of sources, is proportional to r and, due to properties of dipole, is inversely proportional to r squared. Thus, the value of potential generated by the layer is inversely proportional to r. The summarized influence is calculated as an integral by r:

$$P = P_0 \int_{\varepsilon}^{r} \frac{1}{r} dr = P_0(\ln r - \ln \varepsilon)$$

If the distance from electrode to tissue ε is 0.5 mm, the contribution of layers at a distance up to 5 mm will be 33% from summarized contribution of layers up to 100 mm to electrode, e.g. almost all brain volume; if the distance is 10 mm – 56%. Thus, it is possible to claim that we record mainly local activity, although the contribution of local activity is less compared to the conventional method of LFP.

Thus, in the current study we received direct recording of event-related potentials from deep structures, which could be considered as evidence of the activity of the midbrain, in particular PAG.

Cortex-brainstem interaction

Only 5 patients were investigated in the study. This is not enough to receive global data and to have rigorous evidence of only one way of causality. At the same time we have different directions of the links in separate functional states that could be considered a general mechanism of consciousness recovery or disorders.

Studies devoted to animals models postulate that the brainstem and cortex have anatomical and functional connectivity between the midbrain and cortex (Vianna 2001, Sukikara et al. 2006).

We revealed interaction of the cortex and brainstem during awareness (post-anesthesia disorders of consciousness), obnubilation and clear consciousness. Obnubilation is considered as an unstable disorder of consciousness when it is possible to reveal the primary cortex and primary brainstem symptoms. Found changes of connectivity might reflect transitory "vertical" shifts of functional connectivity between the cortex and underlying structures of the brain and varies unstable connectivity could cause a current pathological state.

Only two patients had a short-time period of obnubilation, and we were not able to record ERP in all the patients during each stage of consciousness recovery, so we could not consider the obtained data as global. At the same time the similarity of connectivity detected in the same state in different patients allowed us to suppose that some general mechanisms were revealed.

Numerous studies have used the oddball paradigm with scalp EEG/ERP recording to examine attention-related modulation of cortical activity and search for correlates of cognitive functions (Naatanen and Picton 1987, Polich 2007). We used this paradigm to study functional connectivity between the brainstem and cortex in attention-related modulation of brain activity. Using simultaneous cortex and deep recording, we observed target-specific responses in the brainstem region (PAG) and traced consequence of the activation within the cortex and deep regions.

Some papers revealed consequence of the activation between the subcortical regions and cortex in the P300 time range (Beck et al. 2017).

The revealed dominant effect of the cortex during post-anesthesia disorders of consciousness was a little unexpected. The revealed connectivity probably reflects the beginning of awareness and consciousness recovery when the level of activation is sufficient to establish stable interaction between structures providing arousal and awareness. Supposedly, ERPs were recorded on the time interval when the balance between the arousal effect of the brainstem and the executive effect of the cortex enables awareness, self-recognition and perception of information, e.g. consciousness recovery.

The dominant decrease of top-down information process transfer under anesthesia could be interpreted in the framework of coding theory, assuming the absence of predicting function of the frontal lobe leads to the absence of conscious perception (Wollstadt et al. 2017, Clark 2013, Bastos et al. 2012).

In clear consciousness the strong effect of the brainstem on the frontal lobe was detected. This data is unexpected as the key role of the cortex in perception and processing information and, consequently, in ERP generation is not in doubt. Nevertheless, in our previous studies devoted to ERP during consciousness recovery in patients with brain trauma being in vegetative state, only the combination of the cortex and deep brainstem dipole sources was a positive prognostic factor, whereas the activation of solely cortex regions led to a chronic unconscious state. The dipole analysis of deep sources has many limits and could not be considered as rigorous evidence, but these data have correlation with the anatomical integrity of vertical connectivity. Using DT-MRI, we found that the integrity of not only horizontal – cortex – tracts but also vertical cortex-spinal tracts was strongly correlated with full consciousness recovery (Sharova et al. 1998, Oknina et al. 2011).

Supposedly, in clear consciousness the optimal connectivity level between the cortex and brainstem structures is forming to provide cognitive activity. If the task is simple, the activation of the cortex has no value sufficient to general processing of information as in case of listening to tones without instruction. If the task requires voluntary activity such as attention or memory, the higher level of brainstem activation provides the background where the sustained activity of cortex regions and forming connectivity between cortex areas become possible. The control of activation and connectivity forming is likely to be provided by forward and backward linkage during the task solving.

In this context, the detected changes during the obnubilation could reflect earlier changes of brain activity and reveal the general mechanism of mental disorders. The fact that patients in obnubilation make no mistakes during an active task but the ERP components could not be detected suggests that the cortex has limited resources and could use them keeping consciousness for maximally prolong time. Supposedly, in obnubilation the interrupted activation of the cortex and brainstem with looping cycles of activation and ‘rest’ takes place.

The functional connectivity measures are largely descriptive characteristics. The interpretation of the statistical dependencies between brain regions is not straightforward. The obtained data do not allow highlighting the crucial direction of connectivity to maintain consciousness. But it is possible to postulate that persistent cortex-brainstem connectivity is crucial to awareness and consciousness. For awareness, the detected cortex-brainstem connectivity is supposedly more important; whereas for consciousness maintaining, directed-cortex connectivity.

Thus, the revealed direction of connectivity could reflect the involvement of the midbrain in consciousness and cognition, and the changes in the direction of causality could lead to consciousness disorders. Supposedly, the “vertical”, cortex-subcortex functional connectivity is crucial to maintain consciousness, whereas the “horizontal”, cortex-cortex functional connectivity is important to cognition.

CONCLUSION

The data obtained suppose that the midbrain is involved in high hierarchy processes, such as consciousness and cognition, by the establishment of functional connectivity with the cortex and other subcortical structures. The following changes in direction of functional connectivity were detected during consciousness recovery. The direct connectivity from the frontal area to brainstem was revealed in post-anesthesia disorders of consciousness and obnubilation with a connectivity value greater in post-anesthesia disorders of consciousness; the direct connectivity from the brainstem to left cortical area, in clear consciousness.

ACKNOWLEDGMENT

The study has been supported by RAS and RFFI № 18-013-00967a. Authors’ contribution: Conceived and designed the experiment: DIP, LBO, VVP; performed the experiment: DIP, LBO, VVP, OSZ, analyzed the data: LBO, AOK, ELM, wrote the paper: LBO, ELM, AOK, DIP, OSZ.

Author Disclosure Statement
No competing financial interests exist.

REFERENCES

1. Adams DB. Brain mechanisms for offense, defense and submission. *Behavioral and Brain Sciences*, 1979; 2: 201–41.
2. Bandler R, Keay KA. Columnar organization in the midbrain peri-aqueductal gray and the integration of emotional expression. *Progress in Brain Research*, 1996; 107: 285–300.
3. Bastos AM, Usrey WM, Adams RA, Mangun GR, Fries P, Friston KJ. Canonical microcircuits for predictive coding. Neuron, 2012; 76(4): 695-711.
4. Beck AK, Lutjens G, Schwabe K, Dengler R, Krauss JK., Sandmann P., Thalamic and basal ganglia regions are involved in attentional processing of behaviorally significant events: evidence from simultaneous depth and scalp EEG. *Brain Struct Funct*, 2018; 223(1): 461-474.
5. Blood AJ, Zatorre RJ., Intensely pleasurable responses to music correlate with activity in brain regions implicated in reward and emotion. Proceedings of the National Academy of Sciences, 2001; 98: 11818-11823.
6. Boly XM, Massimini M, Tsuchiya XN, Postle BR, Koch C, and Tononi G., Are the neural correlates of consciousness in the front or in the back of the cerebral cortex? Clinical and Neuroimaging Evidence. *J Neurosci*, 2017; 37(40): 9603–9613.
7. Brandao ML., Anseloni VZ., Pandossio JE., de Araujo JE., Castilho VM., Neurochemical

mechanisms of the defensive behavior in the dorsal midbrain. *Neurosci and Biobehav Rev*, 1999; 23: 863–75.
8. Carrive P, Bandler R, Dampney RA., Somatic and autonomic integration in the midbrain of the unanesthetized decerebrate cat: A distinctive pattern evoked by excitation of neurones in the subtentorial portion of the midbrain periaqueductal grey. *Brain Research*, 1989; 483: 251–58.
9. Clark A., Whatever next? Predictive brains, situated agents, and the future of cognitive science. *Behav Brain Sci*, 2013; 36(03): 181-204.
10. Donchin E., Coles MGH., Is the P300 component a manifestation of context updating? *Behav Brain Sci*, 1988; 11: 357–427.
11. Durschmid S., Zaehle T., Hinrichs H., Heinze H. J., Voges J., Garrido M. I. et al., Sensory deviancy detection measured directly within the human nucleus accumbens. *Cereb Cortex*, 2015; 26: 1–8.
12. Farook JM, Wang Q, Moochhala SM, Zhu ZY, Lee L, Wong PT., Distinct regions of periaqueductal gray (PAG) are involved in freezing behavior in hooded PVG rats on the cat-freezing test apparatus. *Neurosci Lett*, 2004; 354(2): 139-42.
13. Granger CWJ, Investigating causal relations by econometric models and cross-spectral methods. Econometrica, 1969; 37(4): 424-438.
14. Hagmann P., Kurant M., Gigandet X., Thiran P., Wedeen V.J., Meuli R., Thiran J.P., Mapping Human Whole-Brain Structural Networks with Diffusion MRI. *PLoS One*, 2007; 2(7): e597.
15. Herreras O., Local Field Potentials: Myths and Misunderstandings. *Front Neural Circuits*, 2016; 10: 101.
16. Hess WR, Brugger M., Das subkortikale Zentrum der affektiven Abwehrreaktion. *Helvetica Physiologica Acta*, 1943; 1: 33–52.
17. Jasper HH, Introduction. In: Gastaut H., Jasper H., Bancaud J., Waltregny A. eds. The Physiopathogenesis of the epilepsies. Springfield, Illionois: Charles C Thomas, publisher, 1969; 201-8.
18. Kajikawa Y., Schroeder CE., How local is the local field potential? *Neuron*, 2011; 72(5): 847–858.
19. Knight RT, Scabini D, Woods DL, Clayworth CC, Contributions of temporal-parietal junction to the human auditory P3. *Brain Res*, 1989; 502: 109–116.
20. Koch C, Laurent G., Complexity and the nervous system. *Science*, 1999; 284: 96–98.
21. Konovalov AN, Pitskhelauri DI., Principles of treatment of pineal region tumors. *Surg Neurol*, 2003; 59(4): 252-270.
22. Kropotov JD, Ponomarev VA., Subcortical neuronal correlates of component P300 in man. *Electroencephalogr Clin Neurophysiol*, 1991; 78: 40–49.
23. Laughlin SB, Sejnowski TJ., Communication in neuronal networks. *Science*, 2003; 301: 1870–1874.
24. Linnman C., Moulton EA., Barmettler G., Becerra L., Borsook D., Neuroimaging of the periaqueductal gray: state of the field. *Neuroimage*, 2012; 60(1): 505-522.
25. Liu XG, Nachev P, Wang SY, Green A, Kennard C, Aziz T. The Saccade-Related Local Field Potentials of the Superior Colliculus: A Functional Marker for Localizing the Periventricular and Periaqueductal Gray. *J Clin neurophysiol*, 2009; 26(4): 280-287.
26. Loeve M., "Probability Theory", Graduate Texts in Mathematics, 4th edition, Springer-Verlag, 1977; 45: 12.
27. Lonstein J, Stern JM. Role of the Midbrain Periaqueductal Gray in Maternal Nurturance and Aggression: C-fos and Electrolytic Lesion Studies in Lactating Rats. *J Neurosci*, 1997; 17: 3364-3378.
28. Merker B., Consciousness without a cerebral cortex: a challenge for neuroscience and medicine. *Behav Brain Sci*, 2007; 30(1): 63-81; discussion 81-134.
29. Naatanen R, Picton T., The N1 wave of the human electric and magnetic response to sound: a review and an analysis of the component structure. *Psychophysiology*, 1987; 24: 375–425.
30. Nashold BS, Wilson PW, Slaughter DG., Sensations evoked by stimulation in the midbrain of man. *J Neurosurg*, 1969; 30(1): 14-24.
31. Oknina LB, Sharova EV, Zaĭtsev OS, Zakharova NE, Masherov EL, Shekut'ev GA, Kornienko VN, Potapov A.A., Long-latency components (N100, N200 and P300) of acoustic evoked potentials in prediction of mental recovery in severe traumatic brain injury. J. *Voprosy neĭrokhirurgii*, 2011; 3: 19-30.
32. Parsons CE, Young KS, Joensson M., Brattico E, Hyam JA, Stein A. et al., Ready for action: a role for the human midbrain in responding to infant vocalizations. *Soc Cogn Affect Neurosci*, 2014; 9(7): 977-84.
33. Parvizi J., Damasio A., Consciousness and the brainstem. *Cognition*, 2001; 79(1-2): 135-60.
34. Penfield W., The mystery of the mind: a critical study of consciousness and the human brain. Princeton, NY: Princeton University Press, 1975.
35. Philippi CL, Feinstein JS, Khalsa SS, Damasio A, Tranel D, Landini G et al., Preserved self-awareness following extensive bilateral brain damage to the insula, anterior Cingulate, and medial prefrontal cortices. *PLoS ONE*, 2012; 7(8): e38413.
36. Pitskhelauri DI, Konovalov AN, Kopachev DN, Samborsky DI, Melnikova-Pitskhelauri TV. Microsurgical third ventriculostomy with stenting in intrinsic brain tumors involving anterior third ventricle. *World Neurosurg*, 2012; 77(5-6): 785.e3-9.
37. Pitskhelauri DI., Konovalov AN., Kornienko VN., Serova NK., Arutiunov NV., Kopachev DN. Intraoperative direct third ventriculostomy and aqueductal stenting in deep-seated midline brain tumors surgery. *Neurosurgery*, 2009; 64: 256-267.
38. Polich J. Updating P300: an integrative theory of P3a and P3b. *Clin Neurophysiol*, 2007; 118: 2128–2148.

39. Rektor I, Bares M, Kanovsky P, Brazdil M, Klajblova I, Streitova H. et al, Cognitive potentials in the basal ganglia-frontocortical circuits. An intracerebral recording study. *Exp Brain Res*, 2004; 158: 289–301.
40. Scharova E.V., Oknina L.B., Potapov A.A., Zaytsev O.S., Masherov E.L., Kulicov M.A. The P300 component of the acoustic evoked potential in posttraumatic vegetative state of the autonomic nervous system. *Zh Vyssh Nerv Deiat Im I P Pavlova*, 1998; 48(4): 719-730.
41. Schulz GM., Varga M., Jeffires K., Ludlow CL., Braun AR. Functional neuroanatomy of human vocalization: an H215O PET study. Cerebral Cortex, 2005; 15(12); 1835 – 47.
42. Sherwood CC, Subiaul F, Zawidzki TW. A natural history of the human mind: tracing evolutionary changes in brain and cognition. *J Anat*, 2008; 212(4): 426-54.
43. Sherwood CC, Subiaul F, Zawidzki TW. A natural history of the human mind: tracing evolutionary changes in brain and cognition. *J Anat, 2008;* 212(4): 426–454.
44. Strehler BL. Where Is the Self? A Neuroanatomical Theory of Consciousness. *Synapse*, 1991; 7: 44-91.
45. Sukikara MH, Mota-Ortiz SR, Baldo MV, Felício LF, Canteras NS. A role for the periaqueductal gray in switching adaptive behavioral responses. J Neurosci, 2006; 26(9): 2583-9.
46. Tadel F, Baillet S, Mosher JC, Pantazis D, Leahy RM. Brainstorm: A User-Friendly Application for MEG/EEG Analysis *Comput Intell Neurosci*, 2011; 2011: 879716.
47. Taira T., Amano K., Kawamura H., Tanikawa T., Kawabatake H., Notani M., et al. Short latency somatosensory-evoked potentials--direct recording from the human midbrain and thalamus. *Acta Neurochir Suppl*, 1987; 39: 170-3.
48. Verleger R., On the utility of P3 latency as an index of mental chronometry. *Psychophysiology*, 1997; 34: 131–156.
49. Vianna DM., Lesion of the ventral periaqueductal gray reduces conditioned fear but does not change freezing induced by stimulation of the dorsal periaqueductal gray. *Learn Mem*, 2001; 8(3): 164-9.
50. Whitmore NW, Lin SC., Unmasking local activity within local field potentials (LFPs) by removing distal electrical signals using independent component analysis, *Neuroimage*, 2016; 132: 79–92.
51. Wiener N., The theory of prediction. In: Beckenbach, E. (Ed.), Modern Mathematics for Engineers. McGraw-Hill, New York, 1956.
52. Wollstadt P, Sellers KK, Rudelt L, Priesemann V, Hutt A, Frohlich F, et al. Breakdown of local information processing may underlie isoflurane anesthesia effects. *PLoS Comput Biol*, 2017; 13(6): e1005511.
53. Wronka E., Kaiser J., Coenen AML. 2012 Neural generators of the auditory evoked potential components P3a and P3b. *Acta Neurobiol Exp* 72:51–64.
54. Zald DH, Pardo JV. 2002. The neural correlates of aversive auditory stimulation. *Neuroimage*. 2002. 16:746-53.